# Adaptive Notch Filter in Bandwidth as OSG for a PLL

*Luciano Emilio BELANDRIA*[1], *Nancy Alejandra AGUDELO*[1], *Hector BOHORQUEZ*[1], *Joan BERGAS-JANE*[2]

[1]Engineering School, Corporación Universitaria del Meta (UNIMETA), 500001 Villavicencio, Colombia
[2]Center of Technological Innovation in Static Converters and Drives, Department of Electrical Engineering, Polytechnic University of Catalonia, Diagonal 647, 08028 Barcelona, Spain

luciano.belabdria@unimeta.edu.co, nancy.agudelo@unimeta.edu.co, hector.bohorquez@unimeta.edu.co, joan.gabriel.bergas@upc.edu

DOI: 10.15598/aeee.v22i2.5322

Article history: Received Jul 13, 2023; Revised May 06, 2024; Accepted May 27, 2024; Published Jun 30, 2024.


***Abstract.*** *This paper presents a new structure of an Orthogonal Signal Generator for a Phase Locked Loop (OSG-PLL), utilizing an Adaptive Notch Filter (ANF) in bandwidth as the foundation. The ANF employed to generate the orthogonal system within the Phase Locked Loop (PLL), is implemented from the parallel configuration of several Bandpass Filters (BPF), starting from a lattice-structured All-Pass Filter (APF). This approach offers benefits such as simplicity and reduced sensitivity to coefficient rounding in fixed-point Digital Signal Processor (DSP) implementations. The bandwidth changes adaptively by adjusting and achieving the optimization of the filter coefficients. Two adaptation algorithms are proposed, studied, and analyzed, one utilizing Gradient Descent (GD) and another based on Proportional Control of Maximum Error (ME). A series of comparative simulations are conducted using MATLAB software to validate the most effective method among the two described algorithms. The simulation results from MATLAB and the experimental results from a fixed-point digital signal processor (DSP), specifically the TMS320F812, are showcased and examined to assess the effectiveness of the algorithm of proportional control of the ME, which has been selected as the superior alternative, thereby supporting its theoretical development.*

## Keywords

***Adaptive Notch Filter, phase locked loops, orthogonal signal generator, single-phase supply, all-pass filter.***

## 1. Introduction

Currently, the rise in energy consumption and its correlation with the increase in environmental pollutants have prompted many countries to explore a novel energy alternative, known as renewable energy. This type of energy is characterized by its cleanliness and inexhaustible [1]. Ensure stable operation and synchronization of power converters connected to the electrical grid is essential in renewable energy generation systems. The single-phase Phase Locked Loop (PLL) has become a crucial component within grid synchronization methods. The simple implementation, robust, accurate and fast response of the PLL is crucial for control and protection objectives, notably in presence of harmonics and frequency variations [2]. One of the categories into which the PLL is divided, depending of the phase detector implementation, is the PLL based in an Orthogonal Signal Generator (OSG) [3], [4], [5], [6], [7] and [8]. In these PLL's, there are those that present a linearized structure with ANF, equivalent to Park-PLL [9].

In the Infinite Impulse Response (IIR) of Notch Filter (NF), the narrower its bandwidth, the wider will be the transient response and for a higher bandwidth wide

the duration of the transient response can be reduced, however, there will be distortion in the frequency constituents near the notch frequency [10]. In many measurement applications, it is required to have a NF that possesses at same time a very selective magnitude response, (high quality factor Q, low bandwidth) and a short transient response duration. Decrease bandwidth also increases the duration of the transient process in the filter after the action of bias [11].

The IIR of NF, with bandwidth variation, has been used in transient suppression, to remove signals at certain frequency that interfere, for example in the measurement of the Electrocardiographic (ECG) signal [11], [12], [13] and [14], allowing at the filter be more selective within an acceptable level. In ECG signal processing, a basic form of control of the NF bandwidth, is achieved with a variable polar radius [10]. A large polar radius leads to a good speed convergence with a good signal-to-noise ratio (SNR), while a small polar radius allowing a faster filter convergence, but with worse results with respect to the Signal-to-Noise Ratio (SNR) [15]. In the implementation of integrated circuits electronics that work at high frequencies, has also been used the PLL with bandwidth control in a way effective using simple logic control techniques [16], [17] and [18].

In real-time tone detection in the area of information and communication technologies, the ANF has proven to be very effective, being able to adapt not only to the signal frequency, but also to the bandwidth, using an adaptive method based on the Normalized Least Mean Squares (NLMS) [19]. In the elimination of narrow-band interference in the Code Division Multiple Access (CDMA) systems, gradient algorithms have been used for the adaptation of the bandwidth of the NF, resulting in a good SNR and reduced bit error rate [20] and [21]. In the mitigation of interference in Global Positioning System (GPS) receivers, algorithms with Lattice-based notch filters have been developed to adapt the notch frequency along with the bandwidth of the filter [22] and [23].

Bandwidth adaptation is useful in a PLL that is prone to a DC component on your input signal, this is a low frequency error. In order to reduce it, it is required that the bandwidth be extremely low and this would degrade performance dynamic and would not be acceptable if it were kept low and not will return to a higher value [24], [25] and [26].

A new second-order lattice-configured digital IIR NF is presented, whose bandwidth and therefore its quality factor changes in an adaptive way. Two algorithms adapt the bandwidth: one that uses the Gradient Descent (GD) [27], [28] and [29], and another based on the proportional control of the ME. The coefficient $\theta_2$ of an ANF, is adjusted [30], varying the notch bandwidth, obtaining the optimization of the filter coefficients. With the temporary change in the bandwidth value, the transient can be greatly reduced. The effectiveness of the proposal is verified, comparing the performance of both algorithms, using as input sinusoidal signals with unwanted interference. The simulation results and he implementation in a Digital Signal Processor (DSP), show that the algorithms offer a fast speed of convergence, low error, low variation of coefficients of filter and high robustness against disturbances in the signal entrance.

The manuscript is structured in the following manner. In Section 2. , the parallel configuration of second-order bandpass filters is discussed, including its main diagrams and equations. In Sec. 3. , ANF in bandwidth based on GD is presented. In Sec. 4. , ANF in bandwidth with proportional control of maximum error is presented. Section 5. provides comparison of adaptive bandwidth methods. In Sec. 6. , the simulation and implementation results of the fixed-point DSP implementation of the ANF in bandwidth with proportional control of the ME are presented and discussed. Finally, Sec. 7. draws the conclusions.

## 2. Parallel configuration of second-order bandpass filters

In [31], a configuration of an adaptive PLL was presented at the frequency of the single-phase grid, implemented with a single second-order filter. The input signal is formed by the sinusoid at the fundamental frequency, plus the sum of the harmonics, $3^{ero}$, $5^{to}$, $7^{mo}$ y $9^{no}$. To detect and track multiple time-varying frequencies, the options are to use sections made up of a Band Pass Filter (BPF), either in cascade [32] or in parallel. A parallel configuration of second-order BPF sections, justifies the proposed in the independence of the frequency of each section and a common adaptive bandwidth. This basic scheme is illustrated in Fig. 1 for the detection of five sinusoids.

In the application for the case of multiple sinusoids, the using a global error, may result in better accuracy in bandwidth estimation, being sufficient in a higher order problem. Instead, local errors they imply the solution of several problems of insufficient order.

In the configuration of Fig. 1, the corresponding BPF at the fundamental frequency, formed by the All Pass Filter (APF) with lattice configuration, provides the OSG with $x_{1-fund}(n)$ with 90 degrees offset and $x_{2-fund}(n)$ with 0 degree offset, to be used by a Orthogonal Signal Generator for a Phase Locked Loop

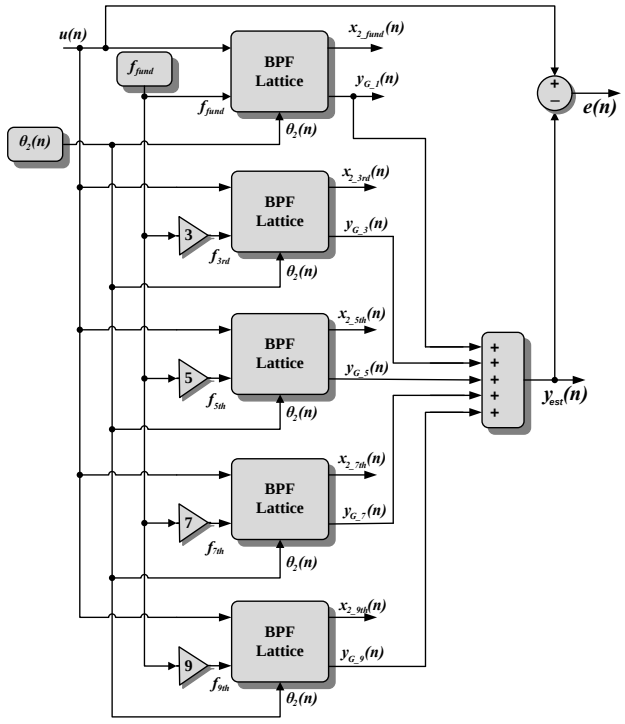


**Fig. 1:** Parallel configuration of second-order BPF's.

(OSG-PLL) [3] and [4], with a common bandwidth for the other filters such that the total estimated output $y_{est}(n)$ is the more similar to the input signal $u(n)$. The output is:

$$\mathcal{Y}_{est}(n) = \sum_{k=1}^{5} \mathcal{Y}_{G\_2k-1}(n) \tag{1}$$

The notch output that is equivalent to the global error is:

$$e(n) = u(n) - \mathcal{Y}_{est}(n) \tag{2}$$

where $\mathcal{Y}_{G\_2k-1}(n)$ corresponds to the output of each BPF tuned to the fundamental frequency and to the frequencies of $3^{ero}$, $5^{to}$, $7^{mo}$ and $9^{no}$ harmonic:

$$\mathcal{Y}_{G\_2k-1}(n) = G_{2k-1}(z)u(n) \tag{3}$$

$$k = 1, 2, .., 5$$

The transfer function of an APF, as mentioned in [30], for each principal sinusoidal component and its harmonics is given by:

$$A_{2k-1}(z) = \frac{\sin\theta_2 + \sin\theta_{1\_2k-1}(1+\sin\theta_2)z^{-1} + z^{-2}}{1 + \sin\theta_{1\_2k-1}(1+\sin\theta_2)z^{-1} + \sin\theta_2 z^{-2}} \tag{4}$$

A BPF from an APF with a lattice structure,answers to:

$$G_{2k-1}(z) = \frac{1}{2}[1 - A_{2k-1}(z)] \tag{5}$$

And therefore, the transfer function of the BPF:

$$G_{2k-1}(z) = \frac{1-\sin\theta_2}{2} \frac{1-z^{-2}}{1 + \sin\theta_{1\_2k-1}(1+\sin\theta_2)z^{-1} + \sin\theta_2 z^{-2}} \tag{6}$$

Also, the NF, from an APF with a lattice structure, responds to:

$$H_{2k-1}(z) = \frac{1}{2}[1 + A_{2k-1}(z)] \tag{7}$$

And therefore, the transfer function of the NF:

$$H_{2k-1}(z) = \frac{1+\sin\theta_2}{2} \frac{1+2\sin\theta_{1\_2k-1}z^{-1}+z^{-2}}{1 + \sin\theta_{1\_2k-1}(1+\sin\theta_2)z^{-1} + \sin\theta_2 z^{-2}} \tag{8}$$

Two methods are proposed, which adapt in the most efficient and simple the common bandwidth of the configuration of Fig. 1, one using the GD [27], [28] and [29], and another new method, easier to implement, based on the proportional control of the ME.

## 3. Adaptive Notch Filter in bandwidth based on Gradient Descent

In [30], [33], [34] and [35] a GD algorithm was used to adapt the value of $\theta_1$ therefore the notch frequency of a second-order IIR NF. Following the same methodology, the value of $\theta_2$ corresponding to the notch bandwidth, is adapted according to the adaptation algorithm:

$$\theta_2(n+1) = \theta_2(n) + \mu e(n)\nabla\theta_2(n) \tag{9}$$

$\mu$ is a positive parameter that controls the adaptation speed of $\theta_2$ in the algorithm. It represents the learning rate, determining how $\theta_2$ is adjusted as a function of the error $e(n)$ and the gradient $\nabla\theta_2(n)$. A high value of $\mu$ accelerates adaptation, but may cause oscillations or divergence. In contrast, a low value of $\mu$ slows down adaptation, providing stability but slower convergence. The choice of $\mu$ is crucial and is determined experimentally to optimize the convergence speed and stability of the adaptive filter.

The value of the filtered regressor of $\theta_2$:

$$\nabla\theta_2(n) = -\frac{\partial e(n)}{\partial\theta_2} = -\frac{\partial[u(n) - y_{est}(n)]}{\partial\theta_2}$$

$$\nabla\theta_2(n) = -\frac{\partial u(n)}{\partial\theta_2} + \frac{\partial y_{est}(n)}{\partial\theta_2}$$

The input signal $u(n)$ does not depend on the parameter $\theta_2$, it is not influenced by the internal parameters of the filter (Parallel configuration of second -order BPF's), as can be seen in Fig. 1. The input signal $u(n)$ comes from the electrical network, therefore, it depends exclusively on the generation and transmission parameters of an alternating current electrical signal, consequently:

$$\frac{\partial u(n)}{\partial \theta_2} = 0$$

Therefore the filtered regressor of $\theta_2$ is:

$$\nabla\theta_2(n) = \frac{\partial y_{est}(n)}{\partial \theta_2} \tag{10}$$

Then the calculation $\nabla\theta_2(n)$ is based on the calculation of the partial derivative of the sums of all BPF outputs with respect to $\theta_2(n)$:

$$\nabla\theta_2(n) = \frac{\partial}{\partial \theta_2}\left[\sum_{k=1}^{5} y_{G\_2k-1}(n)\right], \text{ k=1,2,..,5} \tag{11}$$

$$\nabla\theta_2(n) = \frac{\partial}{\partial \theta_2}\left[y_{G\_1}(n) + y_{G\_3}(n) + y_{G\_5}(n) + y_{G\_7}(n) + y_{G\_9}(n)\right]$$

$$\nabla\theta_2(n) = \frac{\partial y_{G\_1}(n)}{\partial \theta_2} + \frac{\partial y_{G\_3}(n)}{\partial \theta_2} + \frac{\partial y_{G\_5}(n)}{\partial \theta_2} + \frac{\partial y_{G\_7}(n)}{\partial \theta_2} + \frac{\partial y_{G\_9}(n)}{\partial \theta_2} \tag{12}$$

In the case of a single BPF section, the gradient is given by:

$$\frac{\partial y_{G\_2k-1}(n)}{\partial \theta_2} = \frac{\partial G_{2k-1}(z)}{\partial \theta_2} u(n) \tag{13}$$

According to (5) it has to:

$$\frac{\partial y_{G\_2k-1}(n)}{\partial \theta_2} = \frac{1}{2}\left[\frac{\partial}{\partial \theta_2}\left(1 - A_{2k-1}(z)\right)\right] u(n)$$

$$\frac{\partial y_{G\_2k-1}(n)}{\partial \theta_2} = -\frac{1}{2}\frac{\partial A_{2k-1}(z)}{\partial \theta_2} u(n)$$

$$\frac{\partial y_{G\_2k-1}(n)}{\partial \theta_2} = -\frac{\cos\theta_2}{2} \frac{(1-z^{-2})(1+2\sin\theta_{1\_2k-1}z^{-1}+z^{-2})}{(1+\sin\theta_{1\_2k-1}(1+\sin\theta_2)z^{-1}+\sin\theta_2 z^{-2})^2} u(n) \tag{14}$$

Taking into account that:

$$D(z) = 1 + \sin\theta_{1\_2k-1}(1+\sin\theta_2)z^{-1} + \sin\theta_2 z^{-2}$$

$$\cos^2\theta_2 = 1 - \sin^2\theta_2 = (1-\sin\theta_2)(1+\sin\theta_2)$$

Operating the expression (14):

$$\frac{\partial y_{G\_2k-1}(n)}{\partial \theta_2} = -\frac{2}{\cos\theta_2} \frac{(1+\sin\theta_2)}{2} \frac{(1+2\sin\theta_{1\_2k-1}z^{-1}+z^{-2})}{D(z)} \frac{(1-\sin\theta_2)}{2} \frac{(1-z^{-2})}{D(z)} u(n) \tag{15}$$

According to (6) and (8), it is obtained:

$$\frac{\partial y_{G\_2k-1}(n)}{\partial \theta_2} = -\frac{2}{\cos\theta_2} H_{2k-1}(z) G_{2k-1}(z) u(n) \tag{16}$$

The basic scheme that represents the calculation of the gradient of $\theta_2$ for a single lattice filter according to (16), for the case of $k = 1$ corresponding to the fundamental frequency, is illustrated in Fig. 2.

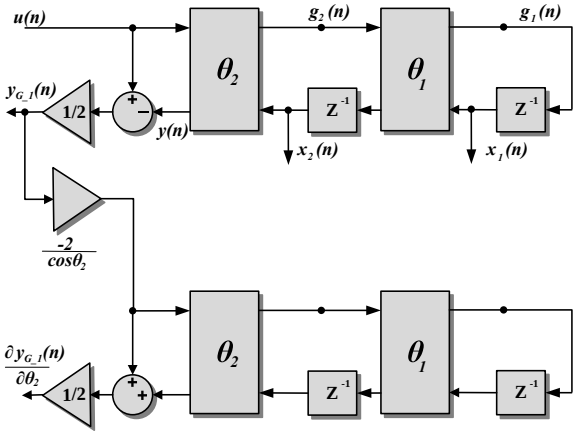


**Fig. 2:** Generation of the gradient of $\theta_2$ for a single lattice filter.

Substituting expression (16) in (12) and using (3), the filtered regressor of $\theta_2$ is obtained for the sums of all outputs of the BPF's:

$$\nabla\theta_2(n) = -\frac{2}{\cos\theta_2}\left[\sum_{k=1}^{5} H_{2k-1}(z)G_{2k-1}(z)\right] u(n)$$

$$\nabla\theta_2(n) = -\frac{2}{\cos\theta_2}\left[\sum_{k=1}^{5} H_{2k-1}(z) y_{G\_2k-1}(n)\right] \tag{17}$$

with $k = 1, 2, .., 5$

The basic scheme of equation (17) is illustrated in Fig. 3.

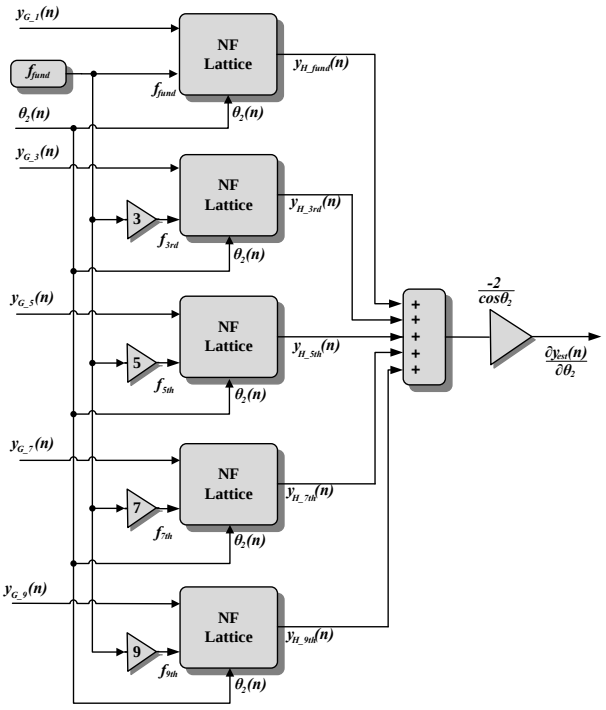


**Fig. 3:** Generation of the gradient of $\theta_2$ for the parallel lattice configuration.

## 4. Adaptive Notch Filter in bandwidth with proportional control of the maximum error

A simple and effective adaptation algorithm is proposed, of the common bandwidth for the BPF's of the configuration in parallel of Fig. 1. This method is primarily based on proportional control of the ME, that is determined. When a fast response is needed due to transients or a sudden change in the input signal $u(n)$, the bandwidth increases quickly. When it is necessary to reject disturbances either by noise o presence of harmonics o no action is needed any more hat the input is a clean signal with no transients, the bandwidth decreases to a minimum value quickly.

The basic principle of the adaptation process has as main advantage that proportional control strategy generates a control signal that is dependent on the error signal. The magnitude of correction increases proportionally with the magnitude of the error, leading to a larger adjustment [36] and [37].

The maximum value of $e(n)$ is achieved when the input signal $u(n)$ has a maximum, which is equivalent to the signal $x_2(n)$ tuned to the fundamental frequency, be maximum, since it is the image of the input and this only happens when the signal $x_1(n)$ zero crossing, due to its orthogonal characteristicwith respect to $x_2(n)$. The algorithm will only update to anew bandwidth value when the error occurs again next zero crossing of the signal $x_1(n)$. The basic outline of the method is illustrated Fig. 4.

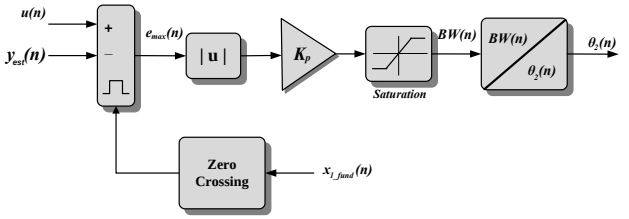


**Fig. 4:** Proportional control of ME.

Bandwidth is determined as:

$$BW(n) = K_p \left| e_{max}(n) \right| \tag{18}$$

The value of the proportional action is establish by the constant Kp. A small value of $K_p$ results in a small proportional action, while a larger $K_p$ leads to a more significant effect. This action can be easily adjusted as it relies on a single parameter. By being proportional to the error, it has the capability to reduce the error, although it may not completely eliminate it in steady-state conditions. Working with the value absolute value of the error, not taking into account its negative value because the bandwidth of the system under study always is greater than zero. Since the lattice BPF's operate with the value of $\theta_2$, it is necessary to convert $BW(n)$ using the expression from [30]:

$$\theta_2(n) = \arcsin\left(\frac{1 - \tan(BW(n)/2)}{1 + \tan(BW(n)/2)}\right) \tag{19}$$

In Fig. 5, the complete scheme of the parallel configuration of the BPF's with the bandwidth adaptation algorithm is presented with proportional control of the ME.

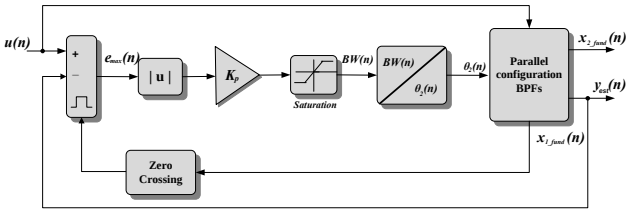


**Fig. 5:** Adaptive algorithm of $\theta_2$ with proportional control of the ME

## 5. Comparison of adaptive bandwidth methods

The methods are compared, using simulations of the structures shown in Fig. 3 and Fig. 5, with an

input signal $u(n)$ consisting of a 50 Hz sinusoid with an amplitude of 1 volt, subjected to three types of disturbances. $BW(n)$ is limited to a maximum value of 50 Hz and at a minimum of 1 Hz, which is sufficient for the normal configuration behavior.

In Fig. 6, at the input at $t = 0.3$ s, it is applied suddenly a voltage drop of 25 %. As value of reference, the IEEE 929-2000 standard [38], specifies that during a voltage decrease of 50 % or lower, the maximum trip duration of the photovoltaic inverter should not exceed 6 cycles. The outputs $x_2(n)$ of both algorithms exhibit a similar response, verifying that after a short transient of less tan 2 cycles, the error (difference between the expected ideal output and the signal $x_2(n)$) is less than 0.1.

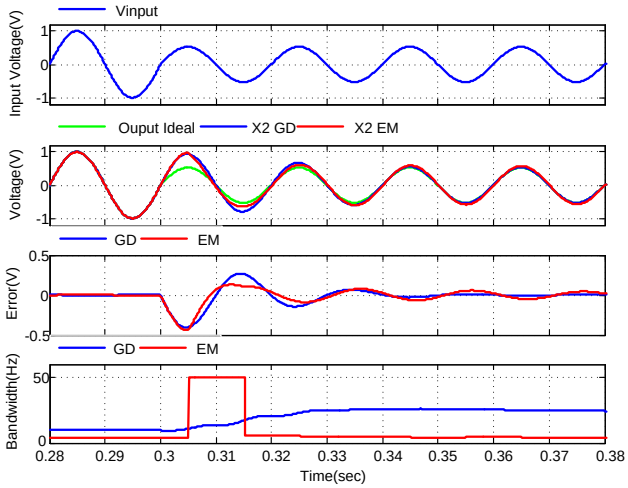


**Fig. 6:** Comparison for a voltage drop.

In Fig. 7, at $t = 0.38$ s, a voltage rise of 15% and sinusoidal harmonics are applied to the input signal, which disappear at $t = 0.5$ s. Both responses are very similar, with significant oscillations in the error within 2 cycles, measuring less than 0.05 V, in the $x_2(n)$ signal of the adaptive algorithm with proportional control of the ME and less than 0.1 V in the GD.

In Fig. 8, at the input signal there is the presence of harmonics all the time and a voltage rise is applied at $t = 0.38$ s, swith a short duration, which disappears at $t = 0.51$ s. The error of the algorithm of proportional control of the ME is smaller (0.05 V) compared to the error of the GD algorithm (0.1 V). The transients are similar and with durations of less than 1.5 cycles.

Using the same disturbance in the case input above, we compare the algorithm of proportional control of the ME with the cases in which there was no adaptation of the bandwidth, as is the case with a small bandwidth and one high, as shown in Fig. 9. Resulting in the error of the adaptive algorithm with proportional control of the ME, it is much less than the other cases, less than 0.05 V, after disappear its transient in 1 cycle.

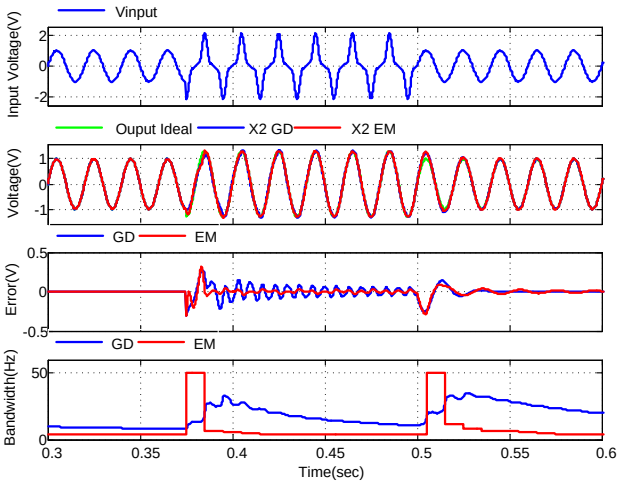


**Fig. 7:** Comparison for voltage rise with harmonics

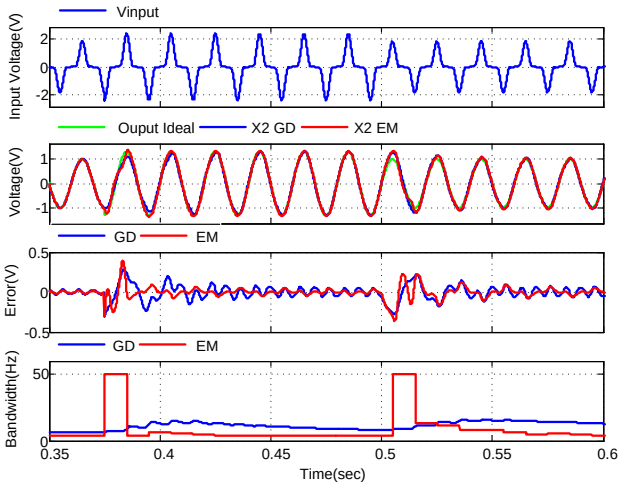


**Fig. 8:** Presence of harmonics and voltage rise.

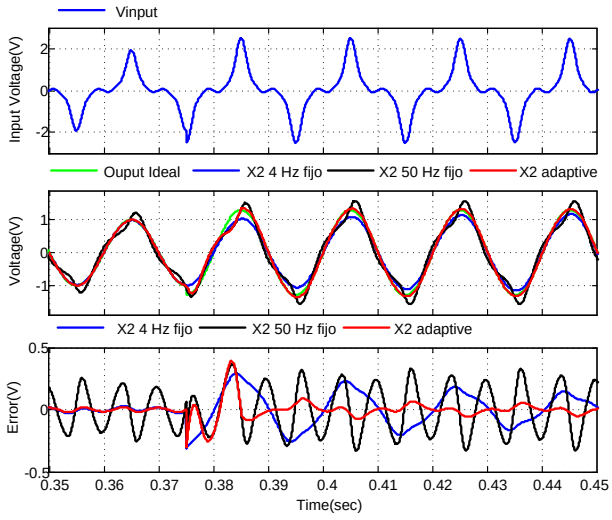


**Fig. 9:** Comparison with small and large bandwidth.

Due to the results and the simplicity of its implementation, which results in a low computational cost,

the algorithm of proportional control of the ME is proposed as the best alternative for adapting the bandwidth $BW(n)$ in a parallel configuration of lattice BPF filters, which generate the necessary OSG for a single-phase PLL.

## 6. Simulation and Experimental Results

To validate the soundness of the theoretical findings put forth in the preceding sections, the ANF in bandwidth with proportional control of ME from Fig. 5, presented in this work, has been simulated with MATLAB and implemented in a DSP from Texas Instruments (TMS320F2812), which has a 32-bit fixed-point CPU with 150 Mips.

The setup consisted of a board with the mentioned DSP, along with a 4-channel, 12-bit Digital-to-Analog Converter (DAC), interfaced with the DSP via the SPI bus; and connected to this DAC, a Picoscope oscilloscope whose graphs are shown in Fig. 10 to Fig. 15

The ANF algorithm is tested, before a series of input signal disturbances [39]. The entries have been generated internally, through mathematical equations. Set of disturbances used, to which they refer in the IEEE Std. 929-2000 [38], suggested guideline for the utility connection of photovoltaic (PV) systems, were the same for simulation and for implementation in DSP.

The variables throughout the simulation and experimental results are: the single-phase input voltage $u(n)$, the signal $x_2(n)$ generated by the BPF tuned to the fundamental frequency and the bandwidth $BW(n)$ provided by the algorithm of proportional control of the ME. The tuning of the ANF remained constant throughout the simulations and implemented in a DSP, with a notch frequency of 50 Hz and a sampling frequency of 20 kHz.

From Fig. 10 to Fig. 15, a thorough congruity can be witnessed between the simulation results and those derived from the execution on a DSP. The ANF, in all instances deployed on the DSP, precisely assesses the output $x_2(n)$ as a reflection of the input signal, devoid of the respective disruptions. Thus, the following analysis of the obtained results corresponds to both the simulation and the DSP implementation, with them exhibiting identical behavior.

The set of disturbances includes:

**Voltage rise**: The input $u(n)$ consists of a 50 Hz sinusoid with a 1.0 pu amplitude. In $t = 0.3$ s, a voltage rise of 80 % is suddenly applied to the input, which disappears 0.3 s later. Fig. 10, shows that, after a short transient, the algorithm successfully aligns the $x_2(n)$ signal with the expected ideal signal within 2 cycles, both when the voltage surge occurs and when it disappears.

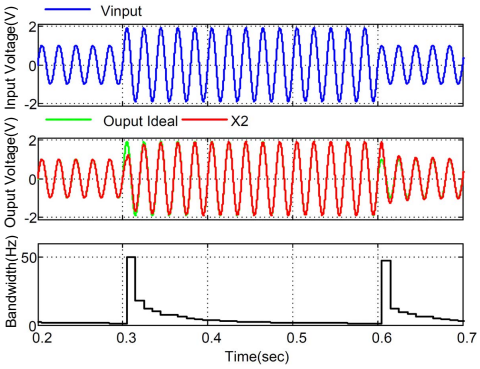


(a) Simulation.

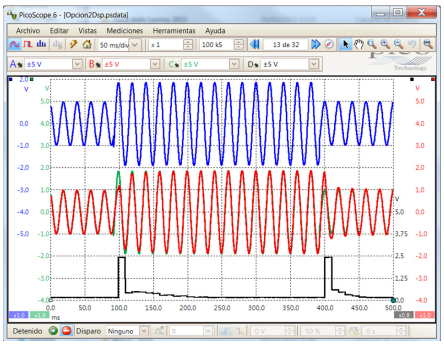

(b) DSP Implementation.

**Fig. 10:** Voltage rise.

**Harmonic distortion**: The proposed algorithm is subjected to a voltage distortion from $t = 0.0$ s, as shown in Fig. 11. The distortion includes 60 % of the $3^{er}$ harmonic, 20 % of the $5^{to}$ harmonic, 12 % of the $7^{mo}$ harmonic, and 3 % of the $9^{no}$ harmonic. The algorithm promptly adapts by minimizing the bandwidth upon detecting the presence of harmonics, causing them to disappear within 0.75 cycles.

**Voltage sag**: At $t = 0.3$ s, a 40 % voltage sag is suddenly applied to the input. The results in Fig. 12 demonstrate that the algorithm increases the bandwidth value to its maximum, so that after a short transient, the $x_2(n)$ signal aligns with the expected ideal signal within 2 cycles, similar to the response observed during the voltage surge.

**Intermittent harmonic distortion**: In Fig. 13, at $t = 0.15$ s, the input is subjected to intermittent harmonic distortion, which disappears after 0.2 s. The algorithm quickly adjusts the bandwidth to eliminate the transient and subsequently reduces it to eliminate the presence of harmonics.

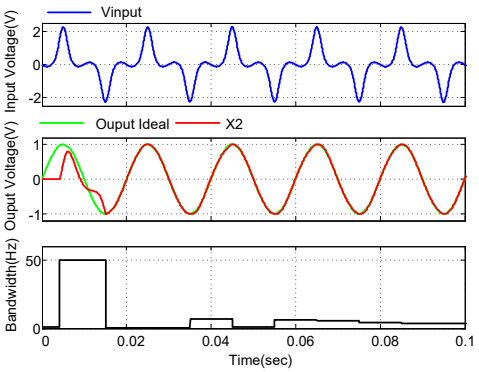


(a) Simulation.

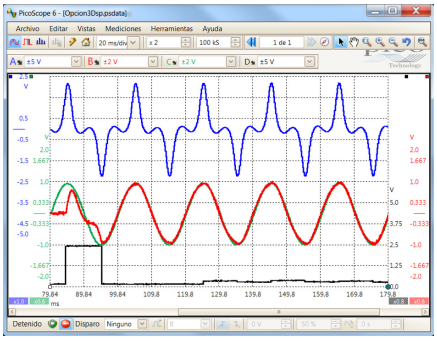

(b) DSP Implementation.

**Fig. 11:** Harmonic distortion.

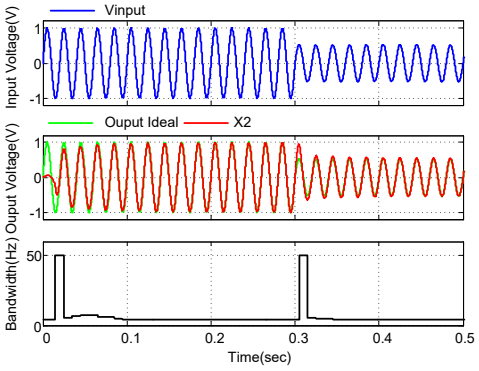


(a) Simulation.

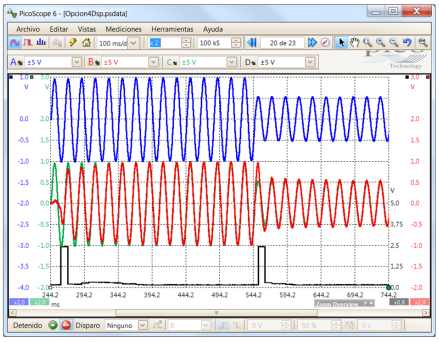

(b) DSP Implementation.

**Fig. 12:** Voltage sag.

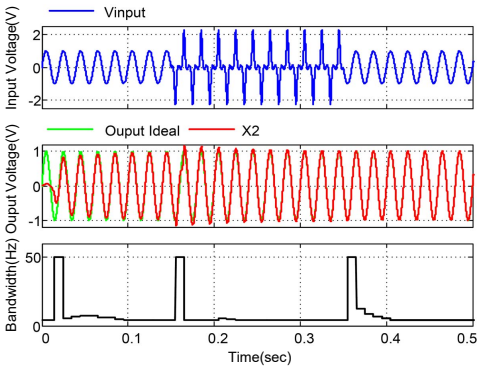


(a) Simulation.

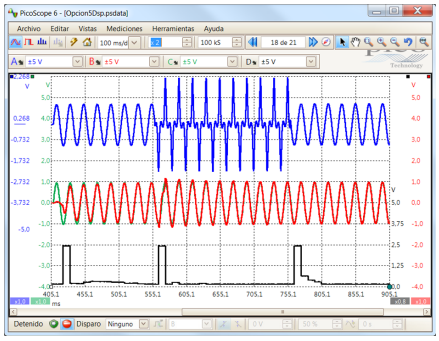

(b) DSP Implementation.

**Fig. 13:** Intermittent harmonic distortion.

**Harmonic distortion with intermittent voltage rise**: This case is similar to the previous one, with the additional presence of a 30 % fundamental voltage surge accompanying the harmonic distortion. Fig. 14 also demonstrates how the algorithm adapts the bandwidth to eliminate both the transient and harmonic distortion.

**Harmonic Distortion with voltage rise**: Fig. 15 illustrates the most extreme case of the studied perturbation, as it involves the presence of harmonics from $t = 0.0$ s, followed by a voltage surge at $t = 0.07$ s. Similar to previous cases, the algorithm adapts the bandwidth by decreasing it to eliminate the harmonics and increasing it to eliminate the transient, enabling the signal $x_2(n)$ to match the expected ideal signal within 0.75 cycles.

## 7. Conclusion

Two adaptation algorithms were presented as an alternative for an OSG in a PLL, using an ANF with bandwidth adaptation based on a parallel configuration of multiple bandpass filters tuned to the fundamental frequency and the frequencies of the $3^{ero}$, $5^{to}$, $7^{mo}$ and $9^{no}$ harmonics. One adaptation algorithm was based on the traditional GD method, while the other

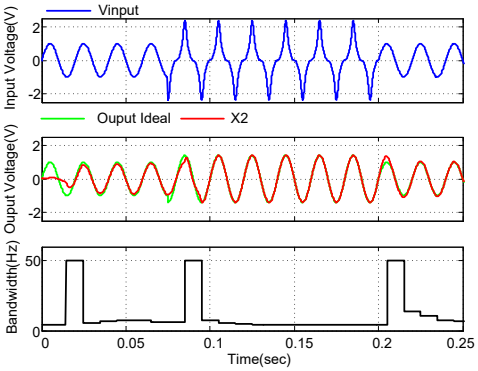


(a) Simulation.

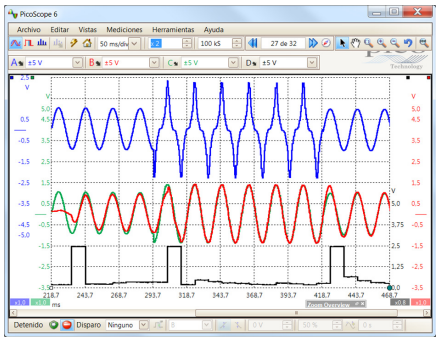

(b) DSP Implementation.

**Fig. 14:** Harmonic distortion with intermittent voltage rise.

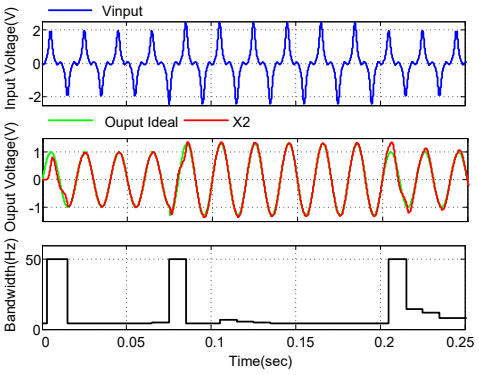


(a) Simulation.

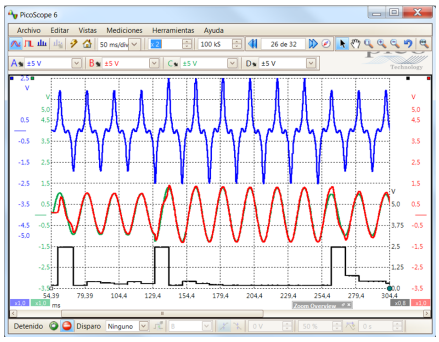

(b) DSP Implementation.

**Fig. 15:** Harmonic Distortion with Voltage Surge.

algorithm was based on a proportional control of the ME that occurs when the orthogonal signal to the input signal crosses zero. This pair of algorithms represents an alternative to classical ANF-based methods. The new algorithms use a global error and a normalized lattice realization. The presented simulations demonstrate good performance of both algorithms when subjected to perturbations in the input signal, characterized by high harmonic content and voltage surges and sags.

They quickly adapt the bandwidth, reducing it to eliminate harmonics and increasing it to reduce transient response times. The algorithm of proportional control of ME, the exhibited better and faster responses than the GD algorithm, further supported by its simplicity in design and implementation, leading to its selection as the main proposal of this work. Simulations and implementation on a DSP confirmed that by utilizing the algorithm of proportional control of ME approach, both the transient duration and the selectivity of the parallel BPF configuration remain at an acceptable level.

# Author Contributions

J. B. and L. B. took the lead in investigating structures of Orthogonal Signal Generators for use in Phase-Locked Loops, based on an Adaptive Notch Filter with bandwidth adaptation. Furthermore, they conceived the original idea, the main conceptual ideas, the overall research objectives, and the design of the implemented algorithms. They were responsible for the direction, supervision, and leadership in the overall planning, test scheme planning, experiments, and research activities. L. B. and N. A. formulated the methodology and theoretical basis, executed analytical computations, orchestrated and executed the simulations. L. B. and H. B. authored the manuscript, including both the initial draft and the final version, with the assistance and input from N. A. and J. B..

L. B. and N. A. executed the model implementation and conducted the experiments. They were actively involved in addressing nearly all technical aspects, performing numerical computations, and conducting measurements for the experiments. N. A. and H. B. conducted data processing and analysis of the experimental results, while also contributing to the graphical representation of the findings. All authors made significant contributions with thorough examination and constructive feedback, which were integrated throughout the entire publication process. They played a crucial role in research design and implementation, executing the experiments, interpreting and analyzing the findings, and actively contributed to the preparation of the manuscript's final version.

## References


[1] ABOUDRAR, I., S. EL HANI, H. MEDIOUNI and A. AGHMADI. Modeling and robust control of a grid connected direct driven PMSG wind turbine by ADRC. *Advances in Electrical and Electronic Engineering*. 2018, vol. 16, iss. 04, pp. 402-413. ISSN 1804-3119. DOI:10.15598/aeee.v16i4.2952.

[2] GHERSIN, A., P. COSSUTTA and M. Aguirre. LPV Control of Current Source Inverter synchronized with the grid. *IEEE Latin America Transactions*. 2020, vol. 18, iss. 10, pp. 1826-1833. ISSN 1548-0992. DOI:10.1109/TLA.2020.9387674.

[3] BELANDRIA, L., N. AGUDELO and J. BERGAS-JANE. Comparative analysis of lattice-based all-pass filter and second order generalized integrator as orthogonal system generator of a pll. *Advances in Electrical and Electronic Engineering*. 2021, vol. 19, iss. 1, pp. 1-15. ISSN 1804-3119. DOI: 10.15598/aeee.v19i1.4002

[4] XU, J., H. QIAN, S. BIAN, Y. HU and S. XIE. Comparative study of single-phase phase-locked loops for grid-connected inverters under non-ideal grid conditions. *CSEE Journal of Power and Energy Systems*. 2020, vol. 8, iss. 1, pp. 155-164. ISSN 2096-0042. DOI: 10.17775/CSEE-JPES.2019.02390

[5] BAMIGBADE, A. and V. KHADKIKAR. Extended State-Based OSG Configurations for SOGI PLL With an Enhanced Disturbance Rejection Capability. *IEEE Transactions on Industry Applications*. 2022, vol. 58, iss. 6, pp. 7792-7804. ISSN 1939-9367.DOI: 10.1109/TIA.2022.3195979

[6] MONTEIRO, L. F., C. FREITAS, M. TCHEOU and D. LESSA. Improvements on E-PLL to Mitigate Transient Low-Frequency Oscillations. *IEEE Latin America Transactions*. 2022, vol. 20, iss. 10, pp. 2244-2253. ISSN 1548-0992. DOI: 10.1109/TLA.2022.9885162

[7] MERAL, M. E. and D. CELIK. DSOGI-PLL Based Power Control Method to Mitigate Control Errors Under Disturbances of Grid Connected Hybrid Renewable Power Systems. *Advances in Electrical and Electronic Engineering*. 2018, vol. 16, iss. 04, pp. 81–91. ISSN 1804-3119. DOI: 10.15598/aeee.v16i1.2485.

[8] ECHCHAACHOUAI, A., S. EL HANI, A. HAMMOUCH and I. ABOUDRAR. A Two-Level Sensorless MPPT Strategy Using SRF-PLL on a PMSG Wind Energy Conversion System. *Advances in Electrical and Electronic Engineering*. 2017, vol. 15, iss. 3, pp. 383–390. ISSN 1804-3119. DOI: 10.15598/aeee.v15i3.2215.

[9] DA SILVA, M., S. FERREIRA, J. DA SILVA, M. DOS SANTOS, A. PAGANOTTI and, L. BARBOSA. Equivalency between adaptive notch filter PLL and inverse park PLL by modeling and parameter adjustment. *IEEE Latin America Transactions*. 2020, vol. 18, iss. 12, pp. 2112-2121. ISSN 1548-0992. DOI: 10.1109/TLA.2020.9400439

[10] TAN, L., J. JIANG and L. WANG. Pole-Radius-Varying IIR Notch Filter with Transient Suppression. *IEEE transactions on instrumentation and measurement*. 2012, vol. 61, iss. 6, pp. 1684–1691. ISSN 0018-9456. DOI: 10.1109/TIM.2012.2184013

[11] PISKOROWSKI, J. Digital Q -varying notch IIR filter with transient suppression. *IEEE transactions on instrumentation and measurement*. 2009, vol. 59, iss. 4, pp. 866-872. ISSN 0018-9456. DOI: 10.1109/TIM.2009.2026605

[12] DECTOR, I. M. and M. A. G. DE ANDA. Parameter-varying notch filter with tunning mechanism for the acquisition of electrocardiographic signals subject to powerline interference. *IEEE Latin America Transactions*. 2015, vol. 13, iss. 4, pp. 943-950. ISSN 1548-0992. DOI:10.1109/TLA.2015.7106341

[13] POMSATHIT, A., P. WATTANALUK, O. SANGAROON, and C. BENJANGKAPRASERT. Variable step-size algorithm for lattice form structure adaptive IIR notch filter. In: *2006 International Conference on Communications, Circuits and Systems*. Guilin: IEEE, 2006. pp. 332-335. ISBN 0-7803-9584-0.

[14] RATHORE, S., A. SHARMA and T. K. RAWAT. Design and Implementation of Time Varying pole Radius IIR Notch filter with improved performance. In: *2nd International Conference on Advances in Computing, Communication Control and Networking (ICACCCN)*. Greater Noida, India: IEEE, 2020. pp. 593-597. ISBN 978-1-7281-8337-4.

[15] MARTIN, J. D. Notch-Ale Adaptive Filter with Varying Pole Radius and Frequency. In: *Fourth International Symposium on Signal Processing and Its Applications*. Gold Coast: IEEE, 1996. pp. 300-303. ISBN 0-7803-4114-7.

[16] KIM, J. Adaptive-bandwidth phase-locked loop with continuous background frequency calibration. *IEEE Transactions on Circuits and Systems II: Express Briefs*. 2009, vol. 56, iss. 3, pp. 205-209. ISSN 1549-7747. DOI: 10.1109/TCSII.2008.2011601

[17] LEE, J. and B. KIM. A low-noise fast-lock phase-locked loop with adaptive bandwidth control. *IEEE Journal of solid-state circuits*. 2000, vol. 35, iss. 8, pp. 1137-1145. ISSN 0018-9200. DOI: 10.1109/4.859502

[18] NIGAM, S., M. MURALI, H. S. GUPTA and S. SAXENA. A 105-525MHz Integer-N Phase-Locked Loop in Indigenous SCL 180nm CMOS. In: *36th International Conference on VLSI Design and 22nd International Conference on Embedded Systems (VLSID)*. Hyderabad, India: IEEE, 2023, pp. 348-352. ISBN 979-8-3503-4679-4.

[19] LIAO, H. E. An oscillator based ANF with adaptable notch-bandwidth for singletone detection. In: *2013 13th International Symposium on Communications and Information Technologies (ISCIT)*. Surat Thani: IEEE, 2013, pp. 374-378. ISBN 978-1-4673-5580-3.

[20] MVUMA, A., S. NISHIMURA and T. HINAMOTO. Adaptive optimization of notch bandwidth of an IIR filter used to suppress narrowband interference in DSSS system. *IEICE transactions on fundamentals of electronics, communications and computer sciences*. 2002, vol. 85, iss. 8, pp. 1789-1797. ISSN 0916-8508. DOI: .

[21] MUUMA, A., S. NISHIMURA and T. HINAMOTO. Adaptive IIR notch filter with controlled bandwidth for narrow-band interference suppression in DS CDMA system. In: *2003 International Symposium on Circuits and Systems (ISCAS)*. Bangkok: IEEE, 2003, pp. 361-364. ISBN 0-7803-7761-3.

[22] ARIF, S. W., A. COSKUN and I. KALE. A Novel Optimization Algorithm for Notch Bandwidth in Lattice Based Adaptive Filter for the Tracking of Interference in GPS. In: *2020 IEEE International Symposium on Circuits and Systems (ISCAS)*. Seville, Spain: IEEE, 2020, pp. 1-5. ISBN 978-1-7281-3320-1.

[23] ARIF, S. W., A. COSKUN and I. KALE. A Fully Adaptive Lattice-based Notch Filter for Mitigation of Interference in GPS. In: *2019 15th Conference on Ph.D Research in Microelectronics and Electronics (PRIME)*. Lausanne, Switzerland: IEEE, 2019, pp. 217-220. ISBN 978-1-7281-3549-6.

[24] SOMKUN, S., S. SRITA, T. KAEWCHUM, A. PANNAWAN, C. SAESEIW and P. PACHANAPAN. Adaptive Notch Filters for Bus Voltage Control and Capacitance Degradation Prognostic of Single-Phase Grid-Connected Inverter. *IEEE Transactions on Industrial Electronics*. 2023, vol. 70, iss. 12, pp. 12190-12200. ISSN 1557-9948. DOI: 10.1109/TIE.2023.3237904.

[25] KANJIYA, P., V. KHADKIKAR and M. S. EL MOURSI. Adaptive Low-Pass Filter Based DC Offset Removal Technique for Three-Phase PLLs. *IEEE Transactions on Industrial Electronics*. 2018, vol. 65, iss. 11, pp. 9025-9029. ISSN 1557-9948. DOI: 10.1109/TIE.2018.2814015.

[26] SMADI, I., I. ATAWI and A. IBRAHIM. Adaptive Low-Pass Filter Based DC Offset Removal Technique for Three-Phase PLLs. *Energies*. 2023, vol. 16, iss. 6, pp. 2873. ISSN 1996-1073. DOI: 10.3390/en16062873.

[27] HAYKIN, S. *Adaptive Filter Theory*. New Jersey: Prentice Hall, 2002. ISBN 13: 9780130901262. ISBN 10: 0130901261

[28] REGALIA, P. A. *Adaptive IIR filtering in signal processing and control*. Boca Raton: CRC Press, 1994. ISBN 13: 978-0824792893. ISBN 10: 0824792890

[29] REGALIA, P. A. An improved lattice-based adaptive IIR notch filter. *IEEE transactions on signal processing*. 1991, vol. 39, iss. 9, pp. 2124-2128. ISSN 1053-587X. DOI: 10.1109/78.134453

[30] BELANDRIA, L. and J. BERGAS-JANE. Single-Phase PLL based on an Adaptive Notch Filter. *Advances in Electrical and Electronic Engineering*. 2020, vol. 18, iss. 3, pp. 169–179. ISSN 1804-3119. DOI: 10.15598/aeee.v18i3.3807.

[31] FANG, X., Y. WANG, M. LI and J. LIUL. A novel frequency-adaptive PLL for single-phase grid-connected converters. In: *2010 IEEE Energy Conversion Congress and Exposition*. Atlanta: IEEE, 2010, pp. 414-419. ISBN 978-1-4244-5286-6

[32] DEBRUNNER, V. and S. TORRES. Multiple fully adaptive notch filter design based on allpass sections. *IEEE transactions on Signal Processing*. 2000, vol. 48, iss. 2, pp. 550-552. ISSN 1053-587X. DOI: 10.1109/78.823981.

[33] MOYA, S E., J. N. J. VILAR, R. A. KORPYS, and J. E. KOLODZIEJ. Frequency and total harmonic distortion estimation based on adaptive filters. *IEEE Latin America Transactions*. 2013, vol. 11, iss. 1, pp. 207-212. ISSN 1548-0992. DOI: 10.1109/TLA.2013.6502804.

[34] REGALIA, P. A. A complex adaptive notch filter. *IEEE Signal Processing Letters* 2010, vol. 17, iss. 11, pp. 937-940. ISSN 1070-9908. DOI: 10.1109/LSP.2010.2075925.

[35] ZHOU, L., H. WEI, Q. JIA and Z. ZHEN. Adaptive PI+ VPI Harmonic Current Compensation Strategy under Weak Grid Conditions. *Ap-*

*plied Sciences*. 2023, vol. 13, iss. 10, pp. 3983. ISSN 2076-3417. DOI: 10.3390/app13105983.

[36] PROAKIS, J. G. and D.v G. MANOLAKIS. *Digital Signal Processing: Principles, Algorithms, and Applications*. New Jersey: Prentice-Hall, Inc., 1996. ISBN 0-13-394-338-9

[37] KUNYA, A. B., M. ARGIN and S. KUCUK-SARI. Optimal Load Frequency Control of Multi-Area Power System Considering Incremental Control Action. In: *IEEE Texas Power and Energy Conference (TPEC)*. College Station, TX, USA: IEEE, 2019, pp. 1-6. ISBN 978-1-5386-9284-4.

[38] IEEE Std 929-2000. *IEEE Recommended Practice for Utility Interface of Photovoltaic (PV) Systems*. IEEE, 2000.

[39] HAN, Y., M. LUO, X. ZHAO, J. M. GUERRERO and L. XU. Comparative Performance Evaluation of Orthogonal-Signal-Generators-Based Single-Phase PLL Algorithms—A Survey. *IEEE Transactions on Power Electronics*. 2016, vol. 31, iss. 5, pp. 3932–3944. ISSN 1941-0107. DOI: 10.1109/TPEL.2015.2466631.

## About Authors

**Luciano Emilio BELANDRIA** was born in Mérida, Venezuela, in 1969. He received the B.S. degree in Electrical Engineering from Universidad de Los Andes (ULA), Mérida, Venezuela, in 1995 and the Ph.D. degree in Electrical Engineering from Polytechnic University of Catalonia (UPC), Barcelona, Spain, in 2015. Since 2001 he has been a professor at the Department of Electronic Engineering at the Universidad del Táchira (UNET), San Cristóbal, Venezuela and since 2021 he has been a professor at the School of Engineering of the Corporación Universitaria del Meta (UNIMETA), Villavicencio, Colombia. His areas of research interest are power electronics, digital motor control, renewable energies, distributed energy resources, voltage and frequency control, and neural networks.

**Nancy Alejandra AGUDELO** was born in San Cristóbal, Venezuela, in 1969. She received the B.S. degree in Electrical Engineering from the University of Los Andes (ULA), Mérida, Venezuela in 1996 and the Ph.D. degree in Electrical engineering from the Polytechnic University of Catalonia (UPC), Barcelona, Spain, in 2015. Since 2001 he has been a professor at the Department of Electronic Engineering at the Universidad del Táchira (UNET), San Cristóbal, Venezuela and since 2021 he has been a professor at the School of Engineering of the Corporación Universitaria del Meta (UNIMETA), Villavicencio, Colombia. Her research interest areas are energy efficiency, energy audits using standard 50001 and electrical installations.

**Hector BOHORQUEZ** was born in Campohermoso, Colombia, in 1950. He received the B.S. degree in Electrical Engineering from the Javeriana University, Bogota, Colombia, in 1975 and Specialized degree in Semiconductors from Institute of Scientific Research, Caracas, Venezuela, in 1985. Since 2021 he has been a professor at the School of Engineering of the Corporación Universitaria del Meta (UNIMETA), Villavicencio, Colombia. His areas of research interest includes industrial electrical installations, semiconductors, virtual instrumentation and renewable energies.

**Joan BERGAS-JANE** was born in Manresa, Spain, in 1970. He received the B.S. degree in industrial engineering and the Ph.D. degree in engineering from the Polytechnic University of Catalonia (UPC), Barcelona, Spain, in 1992 and 2000, respectively. Since 2002, he has been Assistant Professor in the Electrical Engineering Department, Polytechnic University of Catalonia. His research interest lies in the areas of power system quality, power electronics, and digital motor control.

## Appendix A Nomenclature

| | |
|---|---|
| $ANF$ | Adaptive Notch Filter |
| $OSG$ | Orthogonal Signal Generator |
| $PLL$ | Phase-Locked Loop |
| $BPF$ | Bandpass Filter |
| $APF$ | All-Pass Filter |
| $GD$ | Gradient Descent |
| $IIR$ | Infinite Impulse Response |
| $Q$ | Quality factor |
| $SNR$ | Signal-to-Noise Ratio |
| $NLMS$ | Normalized Least Mean Squares |
| $CDMA$ | Code Division Multiple Access |
| $y_{est}(n)$ | Total estimated output |
| $x_1(n)$, $x_2(n)$ | Orthogonal components |
| $e(n)$ | Error global |
| $\mathcal{Y}_{G\_\,2k-1}(n)$ | Output of BPF |
| $A_{2k-1}(z)$ | Transfer function of the APF |
| $G_{2k-1}(z)$ | Transfer function of BPF |
| $H_{2k-1}(z)$ | Transfer function of NF |
| $\theta_2$ | Notch bandwidth coefficient |
| $\nabla\theta_2(n)$ | Filtered regressor value of $\theta_2$ |